

# Point Cloud Semantic Segmentation using Multi Scale Sparse Convolution Neural Network

SuYunzheng  
School of Optics and Photonics  
Beijing Institution of Technology  
BeiJing 100081, China  
suyunzzz@bit.edu.cn

May 12, 2022

## Abstract

Point clouds have the characteristics of disorder, unstructured, and sparseness. Aiming at the problem of the non-structural nature of point clouds, thanks to the excellent performance of convolutional neural networks in image processing, one of the solutions is to extract features from point clouds based on two-dimensional convolutional neural networks. The three-dimensional information carried in the point cloud can be converted to two-dimensional, then processed by a two-dimensional convolutional neural network, and finally back-projected to three-dimensional. In the process of projecting 3D information to 2D and back-projection, certain information loss will inevitably be caused to the point cloud and category inconsistency will be introduced in the back-projection stage; Another solution is the voxel-based point cloud segmentation method, which divides the point cloud into small grids one by one. However, the point cloud is sparse, and the direct use of 3D convolutional neural network inevitably wastes computing resources. In this paper, we propose a feature extraction module based on multi-scale ultra-sparse convolution and a feature selection module based on channel attention and build a point cloud segmentation network framework based on this. By introducing multi-scale sparse convolution, the network could capture richer feature information based on convolution kernels with different sizes, improving the segmentation result of point cloud segmentation.

## 1 Introduction

With the development of stereo matching algorithms and 3D sensors, the importance of point cloud data has become increasingly prominent. The point cloud data contains the three-dimensional coordinates, color, intensity and other information of the scene, which can naturally describe the natural scene. Compared

---

with the two-dimensional image, although the point cloud cannot describe the texture information of the target surface, the three-dimensional point cloud can directly obtain the distance information of the target, which is more in line with our common sense of life. High-quality point cloud data is the bridge between the virtual world and the real world, Through the processing of point cloud data, environmental information can be better perceived, and semantics can enrich the information conveyed by the point cloud. This is of great significance for research directions such as computer vision, intelligent driving, remote sensing mapping, and smart cities.

Point cloud segmentation can determine the shape precisely, category, and other properties of objects of interest in the scene. Taking intelligent driving as an example, as an upstream module, point cloud semantic segmentation needs to segment the ground elements, road signs, and other information based on the point cloud data obtained, to determine the position of the vehicle in combination with the high-definition(HD) maps or perform LiDAR detection([1, 2, 3, 4, 5]). HD maps are a combination of 3D point clouds and relevant semantic information. In the production of HD maps, it is necessary to segment the point cloud map collected by the onboard sensor and then vectorize map elements.

By analogy with 2D image semantic segmentation, point cloud semantic segmentation and 2D image semantic segmentation are similar in definition and are both fine-grained classification of data. Different from 2D images, point clouds are unstructured and have uneven density distribution at different distances. These characteristics make point cloud semantic segmentation more difficult than images. Nevertheless, research in point cloud semantic segmentation has seen an increase in the past few years, a series of point cloud semantic segmentation datasets have emerged, such as semanticKITTI[6]

Unstructured properties and sparsity bring challenges to point cloud semantic segmentation. However, there are many successful methods have been proposed in the literature<sup>2</sup>. For the unstructured nature of point clouds, thanks to the excellent performance of convolutional neural networks in image processing, one of the solutions is to extract features from point clouds based on two-dimensional convolutional neural networks. Through the projection operation, the three-dimensional information can be converted to two-dimensional and then processed by the two-dimensional convolutional neural network, and finally, the result is back-projected to the three-dimensional. In the process of projecting and back-projection, it will cause some information loss inevitably and introduce inconsistency in the back-projection stage. Another solution is to divide the point cloud into voxels, and then use a 3D convolutional neural network to extract features from the point cloud. Although these methods keep the original dimension of the point cloud, the performance and efficiency depend on the voxel-resolution, so it is inevitable to make a trade-off between performance and time-consuming. For the sparsity of point clouds, sparse voxel-based methods reduce computing resource usage and improve efficiency by removing useless computation and memory usage from empty voxel in point cloud, but only single-scale features can be obtained. To better process point cloud in 3D and to take advantage of sparsity, we propose MSSNet, which is built upon

---

MinkowskiEngine[7] and uses multi-scale sparse convolution kernel to extract features with different scales, We summarize the main contributions as:

- Based on the problems of complex preprocessing, poor consistency and easy information loss in point cloud segmentation algorithm, this paper proposed a point cloud segmentation method based on multi-scale sparse convolution.
- In order to fuse point cloud features of different scales, this paper proposes a multi-scale feature fusion method based on attention mechanism. Meanwhile proposes an attention-based feature filter module to avoid the problem of introducing redundant features.
- Through experimental verification, our model can achieve an average intersection ratio of 67.03% on the S3DIS and 66.65% on the SemanticKITTI.

## 2 Related Work

### 2.1 Point-based method

PointNet[8] proposes to use a shared multilayer perceptron to learn point-wise features, and use a symmetric function to learn the global features of the point cloud. The proposed architecture successfully extracts the point-wise feature from irregular and unordered point set. Inspired by PointNet, a series of point-based networks are proposed. Aiming at the problem that PointNet can only learn features point by point and cannot obtain local geometric structure features, PointNet++[9] groups the sampling points in the point cloud, and uses PointNet to extract local features in the local neighborhood of each sampling point, and for the density inhomogeneity of point clouds, multi-scale neighborhood retrieval and multi-resolution neighborhood retrieval are proposed. However, in the preprocess of PointNet and PointNet++, The input point cloud is divided into some  $1m^2$  block with sliding window for semantic segmentation. Therefore they has poor consistency and can not have long range contextual information.

In order to extract the geometric relationship between two points in a local area, PointWeb[10] realizes feature interaction and feature optimization between local points by constructing a dense connection structure locally. Zhang et al.[11] designed a convolutional network based on shell structure. When local feature aggregation in the neighborhood of sampling points is performed, the neighborhood points are divided into different shells according to different radius ranges. Maximum pooling is used to aggregate features, and finally the features of the current center point are obtained through the features of multiple shells.

It should be pointed out that the above-mentioned point-based point cloud segmentation methods all need to perform relatively complex preprocessing on the scene point cloud. In the training phase, the scene point cloud needs to be divided into blocks([8] [9] [10] [11]), this preprocessing method inevitably destroys the consistency of the point cloud.

## 2.2 Projection-based method

Affected by the great success of deep neural networks in the field of 2D computer vision, a natural idea is to reduce the 3D point cloud to 2D, then use mature 2D image semantic segmentation technology to segment it, and then segment the result. Return to 3D space.

Because the method based on multi-view projection([12], [13]) is sensitive to the occlusion and the choice of viewing angle, and suffers from information loss in the process of projection, failing to fully utilize the geometric structure information. Compared with the multi-view projection method, the spherical projection-based method([14], [15]) can retain more information and is more suitable for LiDAR point clouds, but it still suffers from the problems of occlusion and information loss.

## 2.3 Voxel-based method

Dense voxel-based methods ([16], [17]) voxelize the point cloud and directly apply standard 3D convolutions for point cloud semantic segmentation. Although these methods keep the original dimension of the point cloud, the voxelization step inherently introduces discretization artifacts and information loss. Usually, high resolution of voxel leads high memory and computation costs, but low resolution suffers from information loss. It is important to choose an appropriate grid resolution to have a trade-off between segmentation performance and efficiency.

Due to the sparsity of the point cloud, the number of non-zero values after voxelization only accounts for a small percentage. Therefore, it is inefficient to apply dense 3D convolution to the spatially-sparse data. To this end, sparse convolution is proposed([1], [18]), which reduces memory and computational costs by restricting the output of convolution to be only related to active point, which accelerates the computation speed by reducing the useless computation at empty voxels in point cloud. However, affected by voxel-resolution, it is not easy to perceive small-scale objects.

## 2.4 Hybrid method

To further leverage all available information, Hybrid methods are proposed. By fusing point clouds of different representations, such as voxel-based, projection-based and/or point-wise, Hybrid methods obtain richer features and more efficient data processing methods. 3D-MiniNet[19] extract local and global information from point cloud by a learning-based projection module and then utilize a 2D FCNN to generate high-level features to get predictions. PVCNN[20] takes point representation as 3D input data to reduce memory consumption, while convolution in voxels reduces irregular sparse data access and improves locality. SPVNAS[21] replace 3d convolution with sparse convolution, reducing unnecessary computation and improving computational efficiency, authors in SPVNAS[21] use a neural architecture search(NAS)[22] to efficiently design a NN.



As shown in Figure 2, this module arranges the convolution kernels of four scales of large-scale, medium-scale, small-scale and point-level scale in parallel, and captures the features of different scales as  $x_1, x_2, x_3, x_0$  respectively. Among them, the convolution kernel of the point scale level has a convolution kernel size of 1, which means that only linear transformation is performed. This convolution is also called submanifold convolution, which has the characteristics of a small amount of parameters; the feature maps of the other three scales  $x_1, x_2, x_3$  are passed to the feature selection module as the input of the next module.

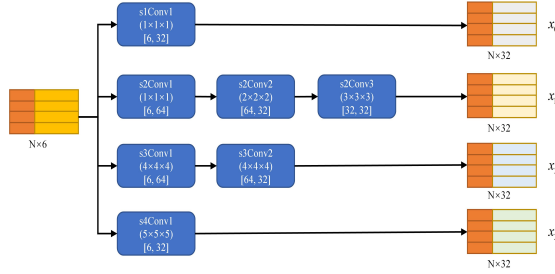


Figure 2: Multi scale feature extract module

### 3.3 Multi Scale Feature Fusion

For the point cloud features output from the multi-scale feature extraction module, our most basic fusion method is to add them, so that the multi-scale features are regarded as the same weight, but in fact, the features of different scales should have the same weight. different influences. As shown in Figure3, inspired by SKNet[25], for the multi-scale features output by the multi-scale feature extraction module. First, the large-scale, medium-scale and small-scale features are added to obtain an intermediate feature map  $X$ , where , and then three different  $MLP$ s are used to perform three transformations on the intermediate feature map  $X$ :

$$\begin{aligned}
 f_1 : X &\rightarrow U_1 \in \mathbb{R}^{N \times 4} \\
 f_2 : X &\rightarrow U_2 \in \mathbb{R}^{N \times 4} \\
 f_3 : X &\rightarrow U_3 \in \mathbb{R}^{N \times 4}
 \end{aligned}
 \tag{1}$$

In the formulal, each transformation function  $f_i$  is a combination of convolution layer, activation function layer and  $BN$  (BatchNormalization) layer. The obtained features of different scales are spliced together and sent to the  $Softmax$  activation function to obtain the score corresponding to each scale:

$$U_{cat} = cat(U_1, U_2, U_3)
 \tag{2}$$

$$Score = softmax(U_{cat})
 \tag{3}$$

### 3.4 Feature Attention Select

In the formula2,  $U_{cat} \in \mathbb{R}^{N \times 3}$  represents the feature map after splicing the features output by formula, and in the formula 3,  $Score \in \mathbb{R}^{N \times 4}$  represents the attention score of each scale. Finally, the multi-scale features are weighted and summed according to their scores to obtain the final multi-scale output. In order to retain the point-by-point scale point cloud characteristics, the input point cloud is subjected to a multi-scale addition after a Submanifold Sparse Convolution with a convolution kernel size of 1 and weighted addition, as the output of the multi-scale feature adaptive fusion module:

$$Output = Conv(x_0 + x_1 \cdot Score[:, 0] + x_2 \cdot Score[:, 1] + x_3 \cdot Score[:, 2]) \quad (4)$$

where  $x_0$  is the output of the Submanifold Sparse Convolution.

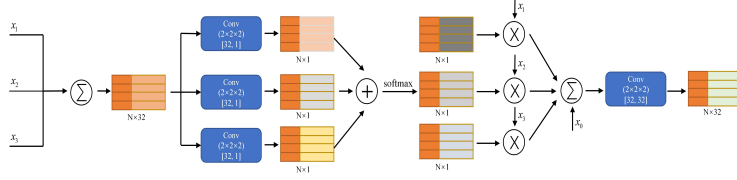


Figure 3: Multi scale feature fusion

### 3.4 Feature Attention Select

In the process of voxel sparse convolution, multiple convolutions are required to continuously extract deep-level features, so the features will become more and more abundant. For convolution operations, the core operation is through multiple convolution layers Superposition to expand the receptive field, so as to perform feature fusion in spatial position. For features in the channel dimension, convolution defaults to adding all channel features. Since it does not consider the importance of different channel features, it will inevitably cause information lost. Inspired by SENet[26] and AF2S3Net[23], as shown in Figure4, the SE-Module is extended to 3D sparse convolution to filter the fused multi-scale features. By optimizing learning, the module can adaptively select features that contribute to the final result, while discarding those that are not important.

Figure 4 shows the feature selection module based on channel attention. For the point cloud feature maps of different scales output by the multi-scale feature extraction module, first process  $x_1, x_2, x_3$  through the residual unit, and the output is recorded as  $x'_1, x'_2, x'_3$ , then connect  $x'_1, x'_2, x'_3$  and introduce nonlinearity. In the SE Module, the input point cloud feature map is passed to global pooling operation to obtain global features:

$$x_c = \frac{1}{N} \sum_{i=1}^N x_i \quad (5)$$

where  $N$  is the voxel number,  $x_i \in \mathbb{R}^{N \times C}$  donate voxel feature.

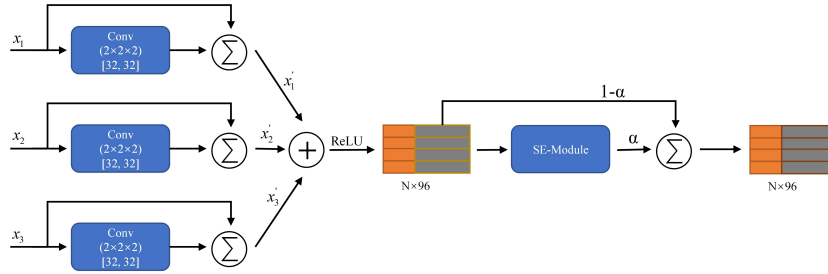


Figure 4: Feature attention select module

For the global features of the point cloud after the Squeeze operation<sup>5</sup>, it is necessary to further obtain the feature relationship between each channel. This step is composed of two linear transformations plus nonlinearity:

$$s = \sigma(W_2\delta(W_1x_c)) \quad (6)$$

where  $\delta$  is the *ReLU* activate function,  $\sigma$  is *Sigmoid* activate function,  $W_1 \in \mathbb{R}^{\frac{C}{r} \times C}$  is the first linear transformation, compress the number of channels from  $C$  to  $\frac{C}{r}$ , reduce the complexity of the model, where  $r$  is the dimension reduction scale factor;  $W_2 \in \mathbb{R}^{C \times \frac{C}{r}}$  is the second linear transformation which restore original number of channels.

Finally, the channel attention coefficients obtained by formula<sup>6</sup> are also weighted on all channels:

$$x_{output} = s_c \cdot x_c \quad (7)$$

where  $s_c$  and  $x_c$  represent the features and weights under different channels,  $s_{output}$  donate the output of SE module. Instead of directly passing through the weighted feature maps as output, we employed a weight factor  $\alpha = 0.6$ , to regularize the weighting effect.

## 4 Network optimization

We leveraged a linear combination of Cross-Entropy loss and lovász-softmax loss<sup>[27]</sup> to optimize our network:

$$L(y, \hat{y}) = w_{ce}L_{ce}(y, \hat{y}) + w_{lovasz}L_{lovasz}(y, \hat{y}) \quad (8)$$

where  $w_{ce}$  and  $w_{lovasz}$  denote the weights of Cross-Entropy loss and Lovász loss respectively. They are both set as 1 in our experiments.

## 5 Experiments

In this section, we share the experimental results to evaluate our model. Section 5.1 briefly explains the experimental datasets. Section 5.3 contains the implementation details. Section 5.4 and Section 5.5 provides the experimental results

of S3DIS[28] and SemanticKITTI[6]. Section 5.6 discuss the advantages of the proposed approach with ablation studies.

## 5.1 Dataset

### 5.1.1 S3DIS

The S3DIS dataset is a large-scale indoor point cloud scene dataset created by Stanford University in 2016. The S3DIS dataset consists of 6 different areas of three buildings used for teaching, each area contains many types of rooms, a total of 271 rooms, each point includes XYZ coordinates, RGB values and is labeled as one of 13 categories. In order to compare with previous methods, 5 regions (1, 2, 3, 4, 6) were used to train our model, and region 5 is used for the comparison of our model’s performance with previous methods.

### 5.1.2 SemanticKITTI

The SemanticKITTI ([6]) dataset is a dataset with point-wise semantic annotations built by the University of Bonn on the basis of the KITTI dataset benchmark, showing traffic in the city center, residential areas, and highway scenes and country roads for outdoor autonomous driving scenarios (Figure 5). The SemanticKITTI dataset provides a total of 28 different categories, 19 of which are used for official algorithm evaluation. As shown in Figure 6, due to the limited sample data, the frequency of some categories is extremely low, such as motorcyclists. The SemanticKITTI dataset was acquired by a Velodyne HDL-64E lidar with a horizontal angular resolution of 0.08 to 0.35, which has 64 vertically scanning beams. The data set includes 22 sequences, with a total of 43551 frames of lidar data, among the driving sequences, 10 sequences (00 to 07, 09 to 10) were used to train our model, and sequence 08 was for the hyperparameter selection. The remaining sequences were used for the comparison of our model’s performance with previous methods.

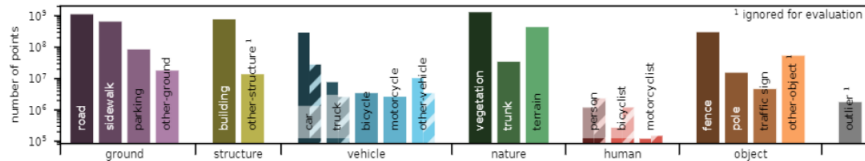


Figure 6: SemanticKITTI class distribution

## 5.2 Evaluation matrix

Confusion matrix is a commonly used method to express classification accuracy. As shown in the Table1, each row of values represents the predicted number of point clouds in the corresponding category after classification, and each column of values represents the actual number of a certain type of point cloud in the

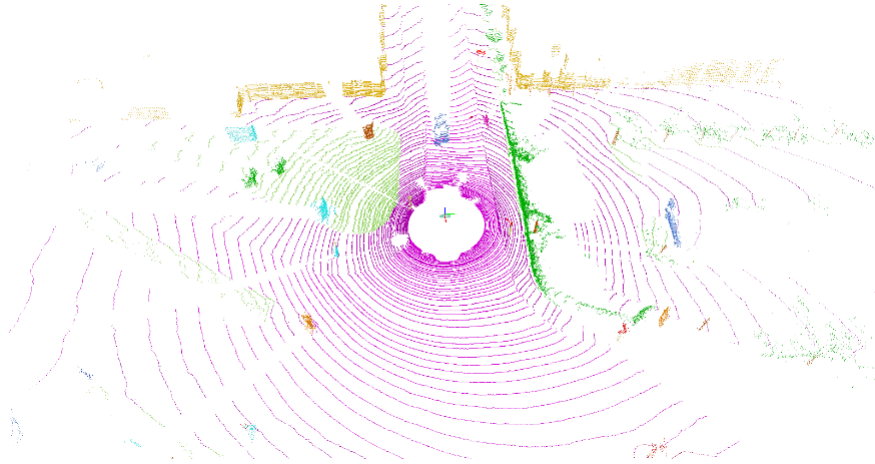


Figure 5: SemanticKITTI

actual type. To evaluate the performance of the proposed method and compare with others, we leverage Intersection over Union (IoU) as our evaluation metric. IoU is the most popular metric for evaluating semantic point cloud segmentation and can be formalized as  $IoU = \frac{TP}{TP+FN+FP}$ , where  $TP$  is the number of true positive points,  $FP$  is the number of false positives, and  $FN$  is the number of false negatives.

Item		Ground truth	
		Positive	Negative
Prediction	Prediction	TP	FP
	Negative	FN	TN

Table 1: Confuse matrix

For the evaluation of multiple categories, the official recommendation of the SemanticKITTI dataset[6] is adopted, and mIoU (mean intersection-over-union ratio) is used as the evaluation metric:

$$mIoU = \frac{1}{C} \sum_{c=1}^C \frac{TP_c}{TP_c + FP_c + FN_c} \quad (9)$$

### 5.3 Implementation details

Those experiments are conducted on two NVIDIA RTX3080Ti GPU. The voxel is a cube shape and its size is 0.05m. At the training step, the proposed model optimized using the Adams optimizer with default parameter setting. Also,  $W_{ce}$  and  $W_{lossz}$  in combined loss function are set to 1.0 and 1.0. Data augmentation

means chosen in this paper are consistent with the paper[7], including random scaling, rotation around the Z axis, spatial translation, and random jittering.

On the S3DIS dataset, the hyperparameters are set as follows: batch size is 2, maximum number of iterations is 150000, initial learning rate is 0.1, and optimizer is Momentum SGD, learning rate adjustment strategy is Poly. On the SemanticKITTI dataset, batch size is 4, maximum number of iterations is 98500, initial learning rate is 0.24, and scheduler is cosine schedule with warmup. At the training phase, the number of input voxels in each scene is limited to 8000.

## 5.4 Evaluation on S3DIS

Table 2 contains a quantitative result of the experiment on S3DIS[28]. From Table 3.2, it can be seen that the PointNet network predicts the test set, and the obtained average intersection ratio mIoU value of semantic segmentation is 43.66, and the average accuracy rate mAcc is 52.63. The PointNet++ network predicts the test set, and the obtained semantic segmentation average accuracy mAcc is 64.22, and the average intersection and union ratio mIoU is 54.36. Compared with PointNet, PointNet++ considers the local information of point cloud, so it can obtain higher mIoU. Compared with PointNet, PointNet++ and other models, this model has a large improvement in IoU for most categories. In the window category, PointNet++ is better than MinkowskiNet and the algorithm in this paper, the main reason for this phenomenon is that PointNet++ performs feature extraction pointwisely. MinkowskiNet and the algorithm in this paper perform voxelization downsampling on the point cloud and then input it into the network, which has a lower resolution than PointNet++. Therefore, on some objects whose geometric features are not particularly obvious, the segmentation effect is slightly worse than that of PointNet++. It should be noted that the preprocess of PointNet and PointNet++ is same, point cloud is cut into blocks, and then randomly selected fixed in each block as the input of network. This processing method will divide the point cloud that is originally an object into different parts as the input of the network. Although the IoU is improved, the consistency of the point cloud segmentation is poor. As shown in Figure 7, different colors represent different categories, the chair in the red box in the figure is partially wrongly segmented into a table by PointNet++. Different from the segmentation of PointNet++ and the preprocessing of randomly sampling fixed points, MinkowskiNet and the algorithm in this paper input the entire room as a sample into the network, for some objects, long-distance context information could be better obtained, therefore, MinkowskiNet and the algorithm in this paper are better than PointNet++ in most categories. Compared with MinkowskiNet, thanks to the help of multi-scale features, the algorithm in this paper has a significant improvement in the IoU of windows, tables, bookshelves, sofas, wooden boards, miscellaneous and other categories.

Figure 8 visualizes some experimental results. From left to right, the RGB scene, the PointNet++ prediction result, the MinkowskiNet prediction result, the algorithm prediction result of this paper and the true value are displayed respectively. As can be seen from the Figure 8, the prediction results of the

## 5.4 Evaluation on S3DIS

Method	Ceiling	Floor	Wall	Beam	Chmn	Window	Door	Chair	Table	Bkcase	Sofa	Board	Clutter	mIoU	mAcc
PointNet	87.4	97.8	71.2	0.0	9.2	52.1	16.3	48.6	58.2	48.3	3.2	39.0	36.2	43.7	52.6
SegCloud	90.1	96.1	69.9	0.0	18.4	38.4	23.1	75.9	70.4	58.4	40.9	13.0	41.6	48.9	57.4
TangentConv	90.5	97.7	74.0	0.0	26.7	39.0	31.3	77.5	69.4	57.3	38.5	48.8	39.8	52.8	60.7
3D RNN	<b>95.2</b>	<b>98.6</b>	77.4	<b>0.8</b>	9.8	52.7	27.9	76.8	78.3	58.6	27.4	39.1	51.0	53.4	71.3
PointNet++	90.7	97.0	75.9	0.0	6.3	<b>58.3</b>	19.4	74.9	69.5	62.2	51.0	57.4	42.9	54.4	64.2
PointCNN	92.3	98.2	79.4	0.0	17.6	22.8	62.1	80.6	74.4	66.7	31.7	62.1	56.7	57.3	63.9
SuperpointGraph	89.4	96.9	78.1	0.0	42.8	48.9	61.6	84.7	<b>75.4</b>	69.8	52.6	2.1	52.2	58.0	66.5
PCCN	90.3	96.2	75.9	0.3	6.0	69.5	63.5	66.9	65.6	47.3	<b>68.9</b>	59.1	46.2	58.3	67.0
MinkowskiNet	92.6	98.2	<b>84.3</b>	0	<b>37.6</b>	51.7	<b>73.8</b>	<b>90.2</b>	73.8	69.7	63.7	66.8	55.3	65.4	72.3
MSSNet(Ours)	91.0	96.2	83.6	0	28.9	56.1	72.7	82.4	74.5	<b>73.1</b>	67.8	<b>76.5</b>	<b>59.9</b>	<b>67.0</b>	<b>74.9</b>

Table 2: Segmentation results of different networks on the S3DIS dataset

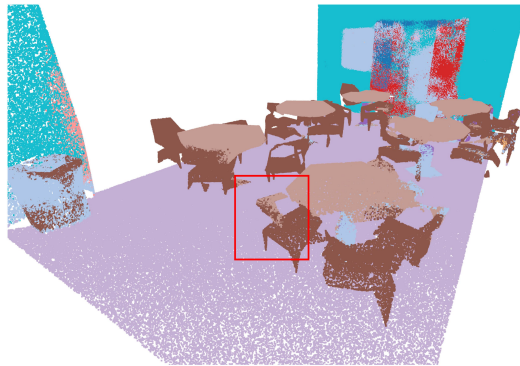


Figure 7: Error segmentation

algorithm in this paper are generally better than those of other algorithms, especially in some categories where the geometric information is not obvious, such as Board, the algorithm in this paper can achieve better segmentation results. Compared with PointNet++, the algorithm in this paper uses the entire room as the input of the network, it can better obtain long-distance context information than PointNet++ network, and for some objects, it is not segmented, so better semantic consistency can be obtained.

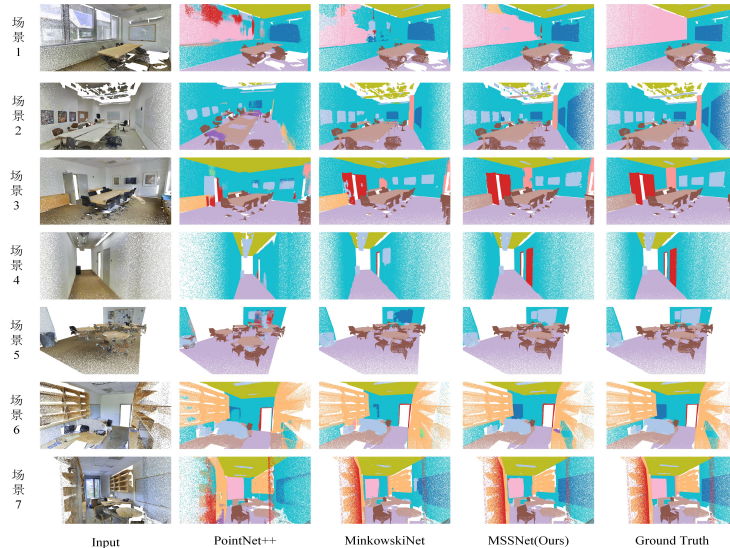


Figure 8: Visualizing the semantic segmentation results of the proposed model using Area5 in S3DIS. The first column is the RGB point cloud, the second column is the prediction of PointNet++, and the third column is the prediction of MinkowskiNet, and the 4-th column is the prediction of the proposed model, and the 5-th column is the ground truth.

## 5.5 Evaluation on SemanticKITTI

SemanticKITTI is an autonomous driving dataset in which the point clouds are all scanned by Velodyne HLE-64E. Compared with the S3DIS dataset, the density of the SemanticKITTI dataset is more uneven.

Table3 is the comparison results of the IoU between the algorithm in this paper and MinkowskiNet and SPVCNN. It can be seen that the algorithm proposed in this paper has the highest mIoU. Compared with MinkowskiNet, the algorithm proposed in this paper has an average cross-union ratio improvement of 4.9%. Benefiting from the multi-scale features, the algorithm proposed in this paper has a significant improvement over MinkowskiNet on some small-scale point clouds, as shown in Table4. By observing Table4, it could be found that for some small-scale objects in the scene, the method proposed in this paper can obtain more accurate segmentation results. For people, bicycles, motorcycles and slightly larger cars in the scene, the IoU is relatively MinkowskiNet has improved greatly.

### 5.5 Evaluation on SemanticKITTI

Method	mIoU(%)
MinkowskiNet	61.1
SPVCNN	63.8
MSSNet(Ours)	<b>66.0</b>

Table 3: Segmentation results of different methods on the SemanticKITTI validation set

Table 5 is the semantic segmentation results of MSSNet using SemanticKITTI test data, it shows the class IoU and mIoU comparison results between our algorithm and other point-based, projection-based, voxel-based and hybrid representation-based segmentation algorithms, bold font indicates the best score in the current category, the results of MinkowskiNet and SPVCNN are the results of the paper[21]. It should be pointed out that other methods in the list may use some additional tricks to improve, while the algorithm in this paper does not use any additional tricks. Through observation, it can be found that the algorithm in this paper has achieved leading results in mIoU and IoU of some small-scale objects (such as bicycles, motorcyclists, poles, etc.).

Method	Person	Bicycle	Bicyclist	Motorcycle	Other vertical
MinkowskiNet	66.9	22.5	82.4	68.6	64.1
SPVCNN	69.7	35.2	82.5	64.6	64.3
MSSNet(Ours)	<b>70.9</b>	<b>44.5</b>	<b>87.7</b>	<b>69.7</b>	<b>66.6</b>

Table 4: Segmentation results of different methods on SemanticKITTI validation set

Method	car	bicycle	motorcycle	truck	other-vehicle	person	bicyclist	motorcyclist	road	parking	sidewalk	other-ground	building	fence	vegetation	trunk	terrain	pole	traffic-sign	mIoU
PointNet	46.3	1.3	0.3	0.1	0.8	0.2	0.2	0.0	61.6	15.8	35.7	1.4	41.4	12.9	31.0	4.6	17.6	2.4	3.7	14.6
RandLA-Net	94.2	26.0	25.8	40.1	38.9	49.2	48.2	7.2	90.7	60.3	71.7	20.4	86.9	56.3	81.4	61.3	66.8	49.2	47.7	53.9
KPCovr	96.0	30.2	42.5	33.4	44.3	61.5	61.6	11.8	88.8	61.3	72.7	31.6	90.5	64.2	84.8	69.2	69.1	56.4	47.4	58.8
SegresNetV3	92.5	38.7	36.5	29.6	33.0	45.6	46.2	20.1	91.7	63.4	74.8	26.4	89.0	59.4	82.0	58.7	65.4	49.6	58.9	55.9
RangNet++	91.4	25.7	34.4	25.7	23.0	38.3	38.8	4.8	91.8	65.0	75.2	27.8	87.4	58.6	80.5	55.1	64.6	47.9	55.9	52.2
SalsaNet	91.9	48.3	38.6	38.9	31.9	60.2	59.0	19.4	91.7	63.7	75.8	29.1	90.2	64.2	81.8	63.6	66.5	54.3	62.1	59.5
PolarNet	93.8	40.3	30.1	22.9	28.5	43.2	40.2	5.6	90.8	61.7	74.4	21.7	90.0	61.3	84.0	65.5	67.8	51.8	57.5	54.3
MinkowskiNet	-	-	-	-	-	-	-	-	-	-	-	-	-	-	-	-	-	-	-	63.1
FusionNet	95.3	47.5	37.7	41.8	34.5	59.5	56.8	11.9	<b>91.8</b>	68.8	77.1	30.8	<b>92.5</b>	69.4	84.5	69.8	68.5	60.4	66.5	61.3
ToradotNet	94.2	55.7	48.1	40.0	38.2	63.6	60.1	34.9	89.7	66.3	74.5	28.7	91.3	65.6	85.6	67.0	<b>71.5</b>	58.0	65.9	63.1
AMVNet	96.2	<b>59.9</b>	<b>54.2</b>	48.8	45.7	<b>71.0</b>	65.7	11.0	90.1	<b>71.0</b>	<b>75.8</b>	<b>32.4</b>	92.4	<b>69.1</b>	<b>85.6</b>	<b>71.7</b>	69.6	62.7	<b>67.2</b>	65.3
SPVCNN	-	-	-	-	-	-	-	-	-	-	-	-	-	-	-	-	-	-	-	63.8
MSSNet(Ours)	<b>96.8</b>	37.8	44.5	<b>50.3</b>	<b>52.1</b>	62.8	<b>75.2</b>	<b>59.8</b>	89.6	65.2	73.1	29.5	91.0	64.7	85.3	71.1	69.6	<b>62.7</b>	63.8	<b>65.5</b>

Table 5: SemanticKITTI Test Leaderboard Results

Figure 9 visualizes the semantic segmentation results of MSSNet. The test sequence is 08 sequence in SemanticKITTI[6]. The first column is prediction of MinkowskiNet and the second column is our predictions. The last column is the visualization of ground truth. As you can see, MinkowskiNet is prone to wrong segmentation for some small-scale objects, the method in this paper benefits from multi-scale feature extraction and fusion, and the ability to perceive small-scale objects is improved. The bicycle in the red circle in scene 1 is divided into other categories by MinkowskiNet, and the algorithm proposed in this paper can achieve the correct segmentation result.

## 5.5 Evaluation on SemanticKITTI

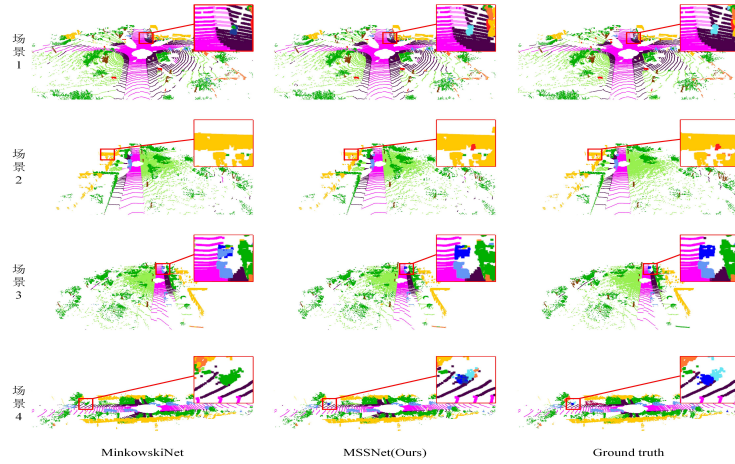


Figure 9: Visualizing the semantic segmentation results of the proposed model using 08 sequence in SemanticKITTI. The first column is the prediction of MinkowskiNet, the second column is the prediction of the proposed model, and the third column is the ground truth. We observe that the proposed model segments well at some small scale objects

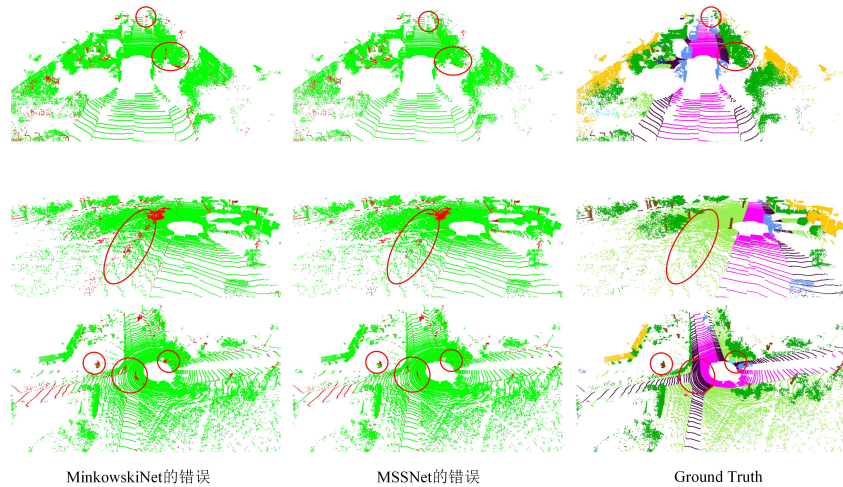


Figure 10: Visualizing the segmentation difference of the proposed model using 08 sequence in SemanticKITTI. The first column is the difference between MinkowskiNet and ground truth, the second column is the difference between MSSNet and ground truth, and the third column is the ground truth. We observe that the proposed model could reduce error segmentation

Figure10 visualizes the semantic segmentation error, The first column is error

prediction of MinkowskiNet and the second column is our error predictions. The last column is the visualization of ground truth. Red color indicates miss-classified points, green color indicates right-classified points. Taking scene 1 as an example, in the part inside the red circle, the segmentation error area of the algorithm in this paper is significantly smaller than that of MinkowskiNet, which proves the effectiveness of the algorithm in this paper.

In order to explain as much as possible that the method in this paper has the property of extracting features at different scales, we visualize the concerns of different scales of convolution kernels. As shown in Figure 11, different sizes of convolution kernels correspond to different colors: green represents the focus of small-scale convolution kernels, dark blue represents the focus of medium-scale convolution kernels, and light blue represents the focus of large-scale convolution kernels. As we can see, The small-scale convolution kernel pays attention to some street signs, the medium-scale convolution kernel pays attention to some poles and some tree trunks, and the large-scale convolution kernel pays attention to the distant street trees and tree trunks. This explains to a certain extent that the multi-scale convolution kernels in this paper can learn features of different scales.

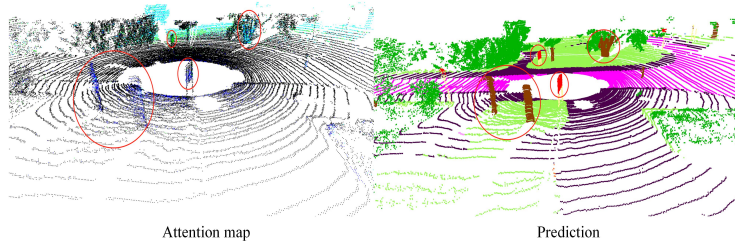


Figure 11: Attention map on SemanticKITTI sequence 08

## 5.6 Ablation studies

In order to verify the functions of different modules of the algorithm in this chapter, ablation experiments are designed on the S3DIS dataset to analyze the effects of multi-scale feature extraction and multi-scale feature fusion. The basic network of this chapter is the U-shaped network after removing the multi-scale feature module and the channel attention-based feature selection module. First train base network using the cross-entropy loss function; Secondly, let the multi-scale feature module only output the fused multi-scale features without feature selection; The features of different scales are not fused, and are directly input into the feature selection module based on channel attention, and the network structure after only adding the feature selection module is obtained. On top of the structure of the basic network, a multi-scale feature module and a channel attention-based feature selection module are added. Finally, the Lovász-softmax

## 5.7 Evaluation by distance

loss function[27] is added to the loss function, and the obtained results are shown in Table6

Observing Table6, we can see that after adding the multi-scale feature module, the mIoU value is increased from 64.33% of the basic network to 66.35%, which shows the importance of multi-scale features. The feature output of three different scales before the fusion is used as the input of the multi-scale feature selection module, the mIoU of the network is 64.50%, compared with the basic network, there is a certain improvement, but the improvement is limited, mainly because the multi-scale features after fusion are not added. If both modules are turned on and the network training is supervised by the cross-entropy loss function, mIoU obtained from the test is 66.47%. Adding the lovász-softmax loss function[27] to the network optimization process, the final average intersection-over-union ratio mIoU is 67.03%. Ablation experiments show that the multi-scale feature extraction and fusion module and the channel attention-based feature selection module proposed in this chapter can improve the multi-scale feature representation ability of the network to improve the segmentation accuracy of the network.

Module	MSFM	FSM	lovász-softmax	mIoU(%)
Baseline				64.33
	✓			66.35
Proposed		✓		64.50
	✓	✓		66.47
	✓	✓	✓	<b>67.03</b>

Table 6: Ablation study of the proposed method vs baseline evaluated on S3DIS validation dataset

## 5.7 Evaluation by distance

In order to verify the robustness of the point cloud scene segmentation algorithm proposed in this chapter, experiments are carried out on SemanticKITTI. In order to show the improvements, we compare MinkowskiNet and SPVCNN on the SemanticKITTI validation set (seq 8). Fig12 illustrates the mIoU of MinkowskiNet, SPVCNN and MSSNet(proposed) with different distance. The results of all the methods get worse by increasing the distance due to the fact that point clouds generated by LiDAR are relatively sparse, specially at large distances. In different regions, the mIoU value of the algorithm proposed in this chapter is always higher than that of SPVCNN and MinkowskiNet, of which MinkowskiNet is the lowest, this is because the SPVCNN algorithm utilizes fine-grained point features, so higher mIoU can be obtained at longer distances. The algorithm proposed in this chapter adds multi-scale features, therefore, it has better segmentation results in each distance range. By analyzing Figure12, it is proved that the algorithm in this chapter has good robustness.

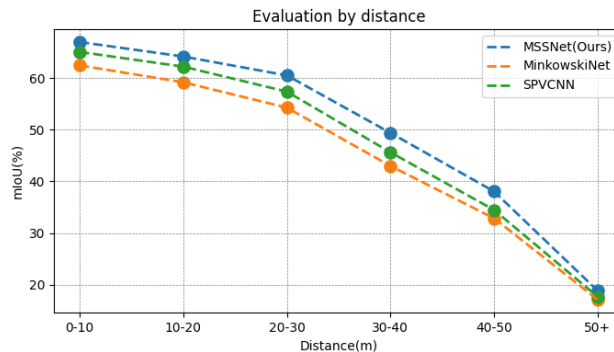


Figure 12: mIoU vs Distance

## 6 Conclusion

In this paper, we proposed MSSNet the multi scale based sparse convolution model for point cloud semantic segmentation. The multi-scale feature extraction module proposed in this chapter uses convolution kernels of different sizes to extract features from the input point cloud to obtain point cloud features of different scales. In order to fuse point cloud features of different scales, this chapter proposes a multi-scale feature fusion module based on attention mechanism. Aiming at the problem that multi-scale features may introduce redundant features, this chapter proposes a feature selection module based on channel attention to filter high-dimensional features. Finally, we conducted the extensive evaluation and discussion of the proposed model using S3DIS and SemanticKITTI, and validated its performance at different distances.

## Acknowledgments

## References

- [1] Yan Yan, Yuxing Mao, and Bo Li. Second: Sparsely embedded convolutional detection. *Sensors*, 18(10):3337, 2018.
- [2] Shaoshuai Shi, Chaoxu Guo, Li Jiang, Zhe Wang, Jianping Shi, Xiaogang Wang, and Hongsheng Li. Pv-rcnn: Point-voxel feature set abstraction for 3d object detection. In *Proceedings of the IEEE/CVF Conference on Computer Vision and Pattern Recognition*, pages 10529–10538, 2020.
- [3] Zhoutao Wang, Qian Xie, Mingqiang Wei, Kun Long, and Jun Wang. Multi-feature fusion votenet for 3d object detection. *ACM Transactions on Multimedia Computing, Communications, and Applications (TOMM)*, 18(1):1–17, 2022.

## REFERENCES

---

- [4] Lue Fan, Ziqi Pang, Tianyuan Zhang, Yu-Xiong Wang, Hang Zhao, Feng Wang, Naiyan Wang, and Zhaoxiang Zhang. Embracing single stride 3d object detector with sparse transformer. *arXiv preprint arXiv:2112.06375*, 2021.
- [5] Alex H Lang, Sourabh Vora, Holger Caesar, Lubing Zhou, Jiong Yang, and Oscar Beijbom. Pointpillars: Fast encoders for object detection from point clouds. In *Proceedings of the IEEE/CVF Conference on Computer Vision and Pattern Recognition*, pages 12697–12705, 2019.
- [6] Jens Behley, Martin Garbade, Andres Milioto, Jan Quenzel, Sven Behnke, Cyrill Stachniss, and Jurgen Gall. Semantickitti: A dataset for semantic scene understanding of lidar sequences. In *Proceedings of the IEEE/CVF International Conference on Computer Vision*, pages 9297–9307, 2019.
- [7] Christopher Choy, JunYoung Gwak, and Silvio Savarese. 4d spatio-temporal convnets: Minkowski convolutional neural networks. In *Proceedings of the IEEE/CVF Conference on Computer Vision and Pattern Recognition*, pages 3075–3084, 2019.
- [8] Charles R Qi, Hao Su, Kaichun Mo, and Leonidas J Guibas. Pointnet: Deep learning on point sets for 3d classification and segmentation. In *Proceedings of the IEEE conference on computer vision and pattern recognition*, pages 652–660, 2017.
- [9] Charles Ruizhongtai Qi, Li Yi, Hao Su, and Leonidas J Guibas. Pointnet++: Deep hierarchical feature learning on point sets in a metric space. *Advances in neural information processing systems*, 30, 2017.
- [10] Hengshuang Zhao, Li Jiang, Chi-Wing Fu, and Jiaya Jia. Pointweb: Enhancing local neighborhood features for point cloud processing. In *Proceedings of the IEEE/CVF conference on computer vision and pattern recognition*, pages 5565–5573, 2019.
- [11] Zhiyuan Zhang, Binh-Son Hua, and Sai-Kit Yeung. Shellnet: Efficient point cloud convolutional neural networks using concentric shells statistics. In *Proceedings of the IEEE/CVF international conference on computer vision*, pages 1607–1616, 2019.
- [12] Maxim Tatarchenko, Jaesik Park, Vladlen Koltun, and Qian-Yi Zhou. Tangent convolutions for dense prediction in 3d. In *Proceedings of the IEEE Conference on Computer Vision and Pattern Recognition*, pages 3887–3896, 2018.
- [13] Felix Järemo Lawin, Martin Danelljan, Patrik Tosteberg, Goutam Bhat, Fahad Shahbaz Khan, and Michael Felsberg. Deep projective 3d semantic segmentation. In *International Conference on Computer Analysis of Images and Patterns*, pages 95–107. Springer, 2017.

## REFERENCES

---

- [14] Andres Milioto, Ignacio Vizzo, Jens Behley, and Cyrill Stachniss. Rangenet++: Fast and accurate lidar semantic segmentation. In *2019 IEEE/RSJ International Conference on Intelligent Robots and Systems (IROS)*, pages 4213–4220. IEEE, 2019.
- [15] Bichen Wu, Xuanyu Zhou, Sicheng Zhao, Xiangyu Yue, and Kurt Keutzer. Squeezesegv2: Improved model structure and unsupervised domain adaptation for road-object segmentation from a lidar point cloud. In *2019 International Conference on Robotics and Automation (ICRA)*, pages 4376–4382. IEEE, 2019.
- [16] Lyne Tchapmi, Christopher Choy, Iro Armeni, JunYoung Gwak, and Silvio Savarese. Segcloud: Semantic segmentation of 3d point clouds. In *2017 international conference on 3D vision (3DV)*, pages 537–547. IEEE, 2017.
- [17] Dario Rehg, Johanna Wald, Jurgen Sturm, Nassir Navab, and Federico Tombari. Fully-convolutional point networks for large-scale point clouds. In *Proceedings of the European Conference on Computer Vision (ECCV)*, pages 596–611, 2018.
- [18] Benjamin Graham, Martin Engelcke, and Laurens Van Der Maaten. 3d semantic segmentation with submanifold sparse convolutional networks. In *Proceedings of the IEEE conference on computer vision and pattern recognition*, pages 9224–9232, 2018.
- [19] Inigo Alonso, Luis Riazuelo, Luis Montesano, and Ana C Murillo. 3d-mininet: Learning a 2d representation from point clouds for fast and efficient 3d lidar semantic segmentation. *IEEE Robotics and Automation Letters*, 5(4):5432–5439, 2020.
- [20] Zhijian Liu, Haotian Tang, Yujun Lin, and Song Han. Point-voxel cnn for efficient 3d deep learning. In *Advances in Neural Information Processing Systems*, 2019.
- [21] Haotian Tang, Zhijian Liu, Shengyu Zhao, Yujun Lin, Ji Lin, Hanrui Wang, and Song Han. Searching efficient 3d architectures with sparse point-voxel convolution. In *European conference on computer vision*, pages 685–702. Springer, 2020.
- [22] Chenxi Liu, Barret Zoph, Maxim Neumann, Jonathon Shlens, Wei Hua, Li-Jia Li, Li Fei-Fei, Alan Yuille, Jonathan Huang, and Kevin Murphy. Progressive neural architecture search. In *Proceedings of the European conference on computer vision (ECCV)*, pages 19–34, 2018.
- [23] Ran Cheng, Ryan Razani, Ehsan Taghavi, Enxu Li, and Bingbing Liu. 2-s3net: Attentive feature fusion with adaptive feature selection for sparse semantic segmentation network. In *Proceedings of the IEEE/CVF conference on computer vision and pattern recognition*, pages 12547–12556, 2021.

## REFERENCES

---

- [24] Hao Fang and Florent Lafarge. Pyramid scene parsing network in 3d: Improving semantic segmentation of point clouds with multi-scale contextual information. *Isprs journal of photogrammetry and remote sensing*, 154:246–258, 2019.
- [25] Xiang Li, Wenhai Wang, Xiaolin Hu, and Jian Yang. Selective kernel networks. In *Proceedings of the IEEE/CVF Conference on Computer Vision and Pattern Recognition*, pages 510–519, 2019.
- [26] Jie Hu, Li Shen, and Gang Sun. Squeeze-and-excitation networks. In *Proceedings of the IEEE conference on computer vision and pattern recognition*, pages 7132–7141, 2018.
- [27] Maxim Berman, Amal Rannen Triki, and Matthew B Blaschko. The lovász-softmax loss: A tractable surrogate for the optimization of the intersection-over-union measure in neural networks. In *Proceedings of the IEEE conference on computer vision and pattern recognition*, pages 4413–4421, 2018.
- [28] Iro Armeni, Ozan Sener, Amir R Zamir, Helen Jiang, Ioannis Brilakis, Martin Fischer, and Silvio Savarese. 3d semantic parsing of large-scale indoor spaces. In *Proceedings of the IEEE conference on computer vision and pattern recognition*, pages 1534–1543, 2016.